VERIFICATION OF PREDICTION MODELS FOR EARLY-AGE AND DRYING SHRINKAGE OF HIGH-PERFORMANCE CONCRETE

Hani H. Nassif, Ph.D., P.E., Nakin Suksawang, and Maqbool Mohamad
Department of Civil and Environmental Engineering, Rutgers University
Piscataway, New Jersey, 08854, USA

ABSTRACT

Early-age properties and their relationships to the long-term durability are important in the quality assurance of high-performance concrete mixes. Moreover, the effects of pozzolanic material, such as fly ash and silica fume, on early-age, as well as drying, shrinkage are not clearly addressed in the available prediction models. The objective of this paper is to present results of a study conducted to identify the early-age (autogenous) and drying shrinkage of normal, as well as lightweight high-performance concrete. The study included an experimental program and a comparison of available analytical models for predicting early age and drying shrinkage. Results from tests performed on different HPC mixes were compared with those from prediction models. HPC mixes were developed and evaluated as part of an overall study for the New Jersey Department of Transportation to develop and implement a mix design and technical specifications for HPC transportation structures.

Results show that fly ash and lightweight aggregate improve the autogenous shrinkage performance of HPC. Moreover, current shrinkage prediction models must be revised to adapt to the HPC mixture.

Keywords: autogenous shrinkage, drying shrinkage, high-performance concrete, pozzolans, fly ash, silica fume, slag, lightweight aggregate

INTRODUCTION

Many State departments of transportation are currently either using high-performance concrete (HPC) or developing new HPC mixes that are suited for transportation structures such as bridge decks. The States that play a leading role in this include Nebraska, New Hampshire, New York, Texas, and Virginia. These States reported success stories with HPC bridge decks. HPC bridge decks exhibited a lower permeability, which leads to a higher concrete durability and increases the concrete service life[1-5]. Nevertheless, HPC is a relatively new material for the industry, and, therefore, more experience and knowledge are needed, especially regarding material handling, placing, and curing methods.

Field observations of recent HPC bridge-deck replacements in various states have raised questions about shrinkage cracking and its causes and remedies—in particular, the early age and the drying shrinkage of HPC. Four main types of shrinkage cracking exist: 1) plastic, 2) carbonation, 3) autogenous (early-age), and 4) drying shrinkage. The plastic and carbonation shrinkage are results of improper pouring sequences and/or schemes, as well as the surrounding environment. Plastic shrinkage occurs when the rate of evaporation exceeds the bleeding rate or, in other words, the concrete dries too fast because of the combination of heat and wind in the surrounding area. Carbonation shrinkage occurs when the cement hydrate reacts with carbon dioxide present in the air. Autogenous shrinkage is associated with the loss of water during the hydration process of the concrete at early-age. Drying shrinkage is the volume change in the concrete as a result of drying. Autogenous shrinkage occurs as soon as the concrete is exposed to air. It is considered relatively small in comparison with drying shrinkage for normal concrete. However, for HPC, autogenous shrinkage contributes significantly to the total shrinkage, and in some cases (e.g., HPC with high-volume silica fume), it could be as high as the drying shrinkage[6-8]. Thus, autogenous shrinkage should no longer be disregarded for HPC.

Moreover, the use of HPC is not limited to the bridge deck construction. HPC is also used in other concrete structures, such as prestressed concrete girders. One of the important calculations for prestressed concrete is the partial loss of prestress. The partial loss of prestress is associated with the shrinkage of concrete. The shrinkage of concrete is predicted using available shrinkage models. However, because the constituents of HPC are very different from those of normal concrete, available models need to be verified for their accuracy and applicability. In this study, the autogenous shrinkage of HPC was investigated. Furthermore, the drying shrinkage results of 61 HPC mixes developed for the New Jersey Department of Transportation (NJDOT) are compared to the results obtained from the available shrinkage prediction models.

EXPERIMENTAL PROGRAM

The experimental program is divided into two phases—drying shrinkage and autogenous shrinkage. The drying shrinkage is used to verify the shrinkage prediction models. The autogenous shrinkage is used for determining the effect of autogenous shrinkage on HPC.

DRYING SHRINKAGE

Drying shrinkage was measured using a length comparator in accordance with ASTM C157. For each mix, three 3- by 3- by 11-in (76.2- by 76.2- by 279.4-mm) prisms were used for determining the average drying shrinkage. The prisms were air dried in a 25- by 16-ft (7.6- by 4.88-m) walk-in environmental chamber with a set temperature and relative humidity of 77°F (25°C) and 50 % relative humidity, respectively. The drying shrinkage was measured at 1, 4, 7, 14, 28, 56, 90, and 180 days.

A total of 61 HPC mixes with a water-to-binder ratio (w/b) ranging from 0.29 to 0.48 were investigated for the drying shrinkage. These HPC mixes were composed of Portland cement type I, ASTM class F fly ash (Sun Ash and Process Ash from Separation Technologies, Inc.), dry, densified silica fume (Force 10,000D from W.R. Grace), 3/8- or 3/4-in. (9.53- or 19.05-mm) crushed stone, concrete sand available locally in New Jersey, and water. Two mixes contained ground-granulated-blast-furnace slag (GBFS) instead of fly ash. In addition, superplasticizer (Daracem 19 from W.R. Grace) and air-entraining agent (Daravair 1000 from W.R. Grace) were added to obtain a slump and air content of 3- to 6-in (76.2- to 152.4-mm) and 4% to 6%, respectively. The placement of concrete was performed in accordance with the general instructions in ASTM C192 using a vibrating table as the method of consolidation. The 28-days compressive strengths for these mixes were also recorded, and they ranged from 6,000- to 10,000-psi (41- to 69-MPa). Furthermore, because the mixes were developed for NJDOT, rapid chloride permeability, scaling, freeze and thaw, elastic modulus, and creep were also performed on selective mixes. Table 2 shows four of the selected mixes used in this study.

AUTOGENOUS SHRINKAGE

Autogenous shrinkage was measured using the same method as drying shrinkage but with a 2-in (50.8 mm) vibrating wire strain gage (VWSG) embedded in the center of the specimens as shown in Fig. 1. The VWSG was selected because of its ability to measure small strains of fresh concrete. Other gages, such as foil gages, usually are restricted by ceramic or other material encasing that protect the foil gage. The VWSG was connected to a Campbell Scientific data logger that collected the strain and temperature data every 10 minutes. The data collection was initiated immediately after the prism was completely cast.

A total of four different mixes—L1, L2, L3 and L4—were investigated to determine the effect of pozzolans on autogenous shrinkage. Table 3 shows the mix proportioning of these mixes. It should be noted that mix L4 uses a 3/4-in (19.05-mm) lightweight aggregate—a shell-type aggregate available from Norlite Co in New York. The lightweight aggregate has a specific gravity of 1.23, unit weight of 50 lb/ft^3 (802.3 kg/m^3), and absorption of 9.1%.

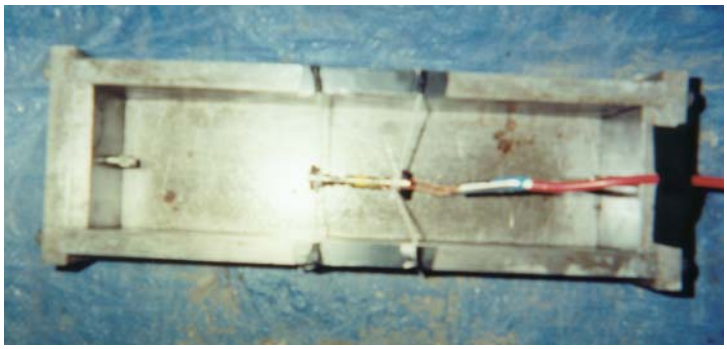

Fig. 1 Embedded Vibrating Wire Strain Gages

	Concrete Mix Design				
	FD2	**FHSC2-1**	**FHSC4-1**	**FHSC2-2**	**FHSC4-2**
Portland Cement Type I (Lb/yd^3)	470	721	844	664	777
Class F Fly Ash (Lb/yd^3)	217	85	162	78	149
Silica Fume (Lb/yd^3)	36	42	76	39	70
3/4" Crushed Stone (Lb/yd^3)	1,871	1,722	1,722	1,871	1,871
Sand (Lb/yd^3)	1,283	1,145	955	1,191	1,015
Water (Lb/yd^3)	289	314	314	289	289
w/b	0.4	0.37	0.29	0.37	0.29
Superplasticizer (oz/cwt)	5	15	22	13	20
AEA (oz/cwt)	1.5	1.5	1.5	1.5	1.5
Slump (in)	3	3	4	3	4
Air Content (%)	3.5	5	3.5	5	3.5
28 days Design Compressive Strength (psi)	6,000	8,000	10,000	8,000	10,000
28 days Shrinkage (%)	0.04	0.04	0.05	0.04	0.05
RCP @ 56 days (Coulomb)	500	800	300	800	300

Table 2 Selective concrete bridge deck and high strength concrete mix proportioning (Note that 1 lb/yd^3 = 0.5933 kg/m^3, 1 in = 25.4 mm, 1 oz/cwt = 65.2 ml/cwt, 1 psi = 0.00689 MPa)

Mix ID	L1	L2	L3	L4
Cement (lb/yd^3)	1082	841	841	1082
Silica Fume (lb/yd3)	120	120	120	120
Fly Ash (lb/yd3)	--	240	--	--
Slag (lb/yd3)	--	--	240	--
Sand (lb/yd3)	767	767	767	523
Gravel (lb/yd3)	1,722	1,722	1,722	868
Water (lb/yd3)	349	349	349	349
SP (oz/cwt)	22	22	22	22
AEA (oz/cwt)	2	2	2	2
Slump (in.)	2.5	8	2	3.5
Air Content (%)	2.5	6.75	2.25	1.75

Table 3 Mix proportion for the autogenous shrinkage test (Note that 1 lb/yd^3 = 0.5933 kg/m^3, 1 in = 25.4 mm, 1 oz/cwt = 65.2 ml/cwt)

AVAILABLE SHRINKAGE MODELS

Five models are considered in this study: 1) ACI Committee 209 model that is adopted by the American Concrete Institute code (ACI 209)[9], 2) CEB-FIP 1990 shrinkage prediction model (CEB 90)[10], 3) Bazant B3 Model (B3)[11–13], 4) Gardner and Lockman GL 2000 model (GL 2000)[14], and 5) Miyazawa and Tazawa model (M&T)[15]. The input factors for all five models are summarized in Table 4.

	ACI 209	CEB 90	B3	GL 2000	M&T
Relative Humidity	Yes	Yes	Yes	Yes	Yes
Specimen Size	Yes	Yes	Yes	Yes	Yes
Specimen Shape			Yes		
Compressive Strength @ 28 days		Yes	Yes	Yes	
Cement Type		Yes	Yes	Yes	
w/c ratio					Yes
Curing Type	Yes		Yes		
Age at the end of Curing	Yes		Yes	Yes	
Slump	Yes				
Fine Aggregate Content	Yes				
Cement Content	Yes				
Air Content	Yes				
Total Parameters	8	4	7	5	3

Table 4 Input factors for Shrinkage Prediction Models

ACI 209 MODEL

The ACI 209 model is based on a shrinkage model proposed by Branson and Christiason[16]. This model has been incorporated in most building codes in the United States, as well as other countries. It is a general-purpose model and does not set any limitation on the strength of the concrete. However, one of the criteria is that the concrete must be moist-cured for a minimum of 7 days or steam-cured for 1 to 3 days. Furthermore, the model is only applicable to type I and III Portland cement.

The model takes into account the relative humidity, the specimen size, the curing type, and the age at the end of curing. The ACI 209 equation for predicting unrestrained shrinkage strain at any time is given by:

$$_{sh\ t} \quad \frac{t}{t} \quad _{sh\ u} \tag{1}$$

$$_{sh\ u} \quad 780 \ _{sh} \quad 10^{\ 6} \tag{2}$$

where:

t = time after which shrinkage is considered (days)
η = 35 for shrinkage of moist-cured concrete after 7 days, and
= 55 for shrinkage of steam-cured concrete after 1 to 3 days
$(\varepsilon_{sh})_u$ = ultimate shrinkage strain (in/in)
γ_{sh} = the product of applicable correction factors that are associated with relative humidity, specimen size, slump, fine-aggregate percentage, cement content, and air content.

CEB 90 MODEL

The CEB 90 model is adopted by the CEB-FIP Model Code 1990 (Euro-International Concrete Committee and International Federation for Prestressing) based on the work by Muller and Hillsdorf[17]. The model is only applicable for concrete with a 28-day compressive strength between 2,900 to 13,000 psi (20 to 90 MPa). The input parameters of this model differ from those of the ACI 209 model in compressive strength and type of curing method. The ACI 209 model does not consider the 28-day compressive strength whereas the CEB 90 model considers only dry curing. The model is given by:

$$\varepsilon_{cs}(t,t_s) = \varepsilon_{cso}.\beta_s(t-t_s) \tag{3}$$

where:

ε_{cso} = notional shrinkage coefficient which is associated with relative humidity, cement type, and compressive strength (in/in)
β_s = coefficient describing the development of shrinkage with time, which is associated with drying time and specimens size
t = age of concrete (days)

t_s = age of concrete at the beginning of the shrinkage (days)

B3 MODEL

The B3 model is the latest edition of a number of shrinkage prediction models developed by Bazant et al[10-12]. A previous version of this model, called BP model, was proposed as early as 1978. It is then modified and renamed to BP-KX Model. The current model is a simpler form of the expanded BP-KX model.

The input parameters in this model are relative humidity, specimen size, specimen shape, 28-day compressive strength, cement type, curing type, and age at the end of curing. The shrinkage strain is calculated using the following equation:

$$_{sh} \quad _{sh} \; k_h S \; t \tag{4}$$

$$S \; t \quad \tanh \; \frac{t \quad t_c}{_{sh}} \; ^{1/2} \tag{5}$$

$$_{sh} \quad 190.8 t_c \; ^{0.08} \; f_c^{'} \; ^{0.25} \; 2k_s \; V/S \; ^{2} \tag{6}$$

where:

$_{sh}$ = time dependence of ultimate shrinkage associated with water content, cement type, curing condition, and compressive strength (in/in)

k_h = humidity dependence associated with relative humidity

t_c = age of concrete curing (days)

t = age drying commenced, end of moist curing (days)

f'_c = concrete compressive strength at 28 days (psi)

k_s = cross-section–shape correction factor (1.25 for infinite square prism)

V/S = volume to surface ratio (in)

GL 2000 MODEL

The GL 2000 model is a modified version of the GZ model proposed by Gardner et al[18]. This model is based on the CEB 90 model, but the GL 2000 model includes the type of cement as one of its input parameter. The input parameters of this model are relative humidity, specimen size, 28-day compressive strength, cement type, and age at the end of curing. The shrinkage strain is calculated using the following expression:

$$_{sh} \quad _{shu} \quad h \quad t \tag{7}$$

where

ε_{shu} = ultimate shrinkage strain associated with compressive strength and cement type (in/in)
$\beta(h)$ = correction term for effect of humidity
$\beta(t)$ = correction term for effect of time associated with specimen size and curing time.

M&T MODEL

Miyazawa and Tazawa[15] proposed two models for the prediction of autogenous and drying shrinkage, respectively. Both models are based on the CEB 90 model and could be applied to high- and normal-strength concrete with a w/c ratio as low as 0.20. For autogenous shrinkage, the model considers the w/c ratio and cement types by applying correction coefficients. For drying shrinkage, the rate of relative humidity is also added to the correction coefficients.

Autogenous Shrinkage:

$$_{c}\ t \qquad _{c0}\ w/c \quad _{a}\ t \tag{8}$$

For $0.2 \le \mathrm{w/c} \le 0.5$:

$$_{c0}\ w/c \quad 3070 \exp \quad 7.2\ w/c \tag{9}$$

For $0.5 < \mathrm{w/c}$:

$$_{c0}\ w/c \quad 80 \tag{10}$$

$$_{a}\ t \quad 1 \quad \exp \quad a\ t \quad t_0\ ^{b} \tag{11}$$

where

$\varepsilon_c(t)$ = autogenous shrinkage of concrete at age t (in/in)
γ = coefficient describing the effect of cement type (1.0 for ordinary Portland cement)
$\varepsilon_{c0}(w/c)$ = ultimate autogenous shrinkage (in/in)
$\beta_a(t)$ = coefficient describing the development of autogenous shrinkage with time
w/c = water-to-cement ratio
a, b = constants depending on water-cement ratio
t = age of concrete (days)
t_0 = initial setting time (days)

Drying Shrinkage:

$$\varepsilon_d(t,t_d) = \varepsilon_{d0}(RH)\beta_d(t) \tag{12}$$

$$_{d0}\ RH \quad e\,1 \quad \exp \quad RH \quad RH_0 \Big/ t_1 \tag{13}$$

$$_{d}\ t \quad \frac{t \quad t_d \Big/ t_1}{350\ h \Big/ h_0 \quad ^2 \quad t \quad t_d \Big/ t_1}^{0.5} \tag{14}$$

$$h = 2A_c \Big/ u \tag{15}$$

where

$\varepsilon_d(t,t_d)$	= drying shrinkage from age t_d to t (in/in)
$\beta_d(t)$	= coefficient describing the development of drying shrinkage with time
$\varepsilon_{d0}(RH)$	= ultimate drying shrinkage (in/in)
t_d	= age of concrete at the start of exposure to the atmosphere (days)
RH	= ambient relative humidity (%) $(40\% \le RH \le 90\%)$
RH_0	= specific relative humidity (%) depending on water-cement ratio
e	= coefficients depending on water-cement ratio
A_c	= cross-sectional area,
u	= perimeter of the member in contact with the atmosphere $(3.93in(100mm) \le h \le 19.68in(500mm)$
h_0	= 3.93-in (100-mm).
t_1	= 1 day

RESULTS AND DISCUSSION

This study has two main objectives—model verification of drying shrinkage and the effect of autogenous shrinkage on HPC. The first objective is to evaluate the accuracy of the shrinkage prediction models in comparison with the measured and collected shrinkage data. The data bank collects shrinkage data from 61 HPC mixes; a total of 345 data points are used for evaluating the models. The second objective is to determine the effect of autogenous shrinkage on HPC. The HPC mixes consist of mixes with a low w/b ratio and a different percentage of pozzolanic material.

MODEL VERIFICATION

Several statistical methods, which can be used for evaluating the accuracy of the models are available. In this paper, a comparison of the predicted shrinkage strains versus the corresponding measured shrinkage strains for the best-fit solution and the degree of scatter are considered. Figs. 2 through 5 show the plots of all five shrinkage prediction models. The solid line represents a perfect correlation between the predicted and measured strains. According to the figures, the B3 model has the least deviation, followed by the GL 2000, ACI 209, CEB 90, and M&T models. The GL 2000 and ACI 209 models are also good shrinkage prediction models for HPC. The CEB 90 and M&T models have poor shrinkage-prediction value and, therefore, should not be used to predict the shrinkage for HPC.

It is also observed that, in general, with the exception of the ACI 209 model, the models overpredicted the drying shrinkage at early ages and underestimated the drying shrinkage at later ages. The ACI 209 model always underpredicts the drying shrinkage of HPC because the model is based on the shrinkage value of 7-day moist-cured specimens whereas the test specimens are dry-cured; this leads to a higher shrinkage strain.

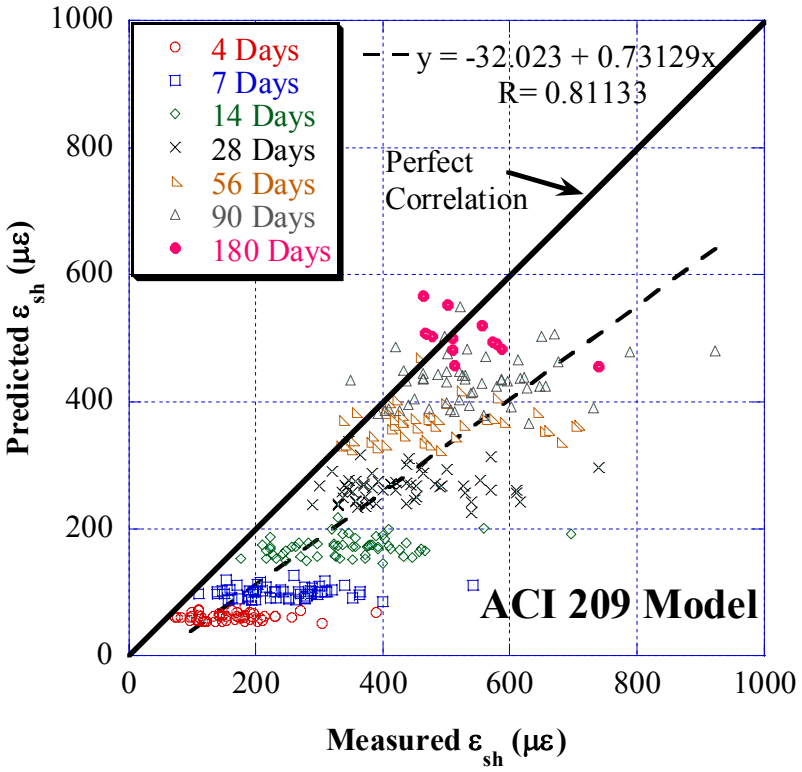

Fig. 2 Comparison of Predicted and Measured Shrinkage Strains for ACI 209 Models

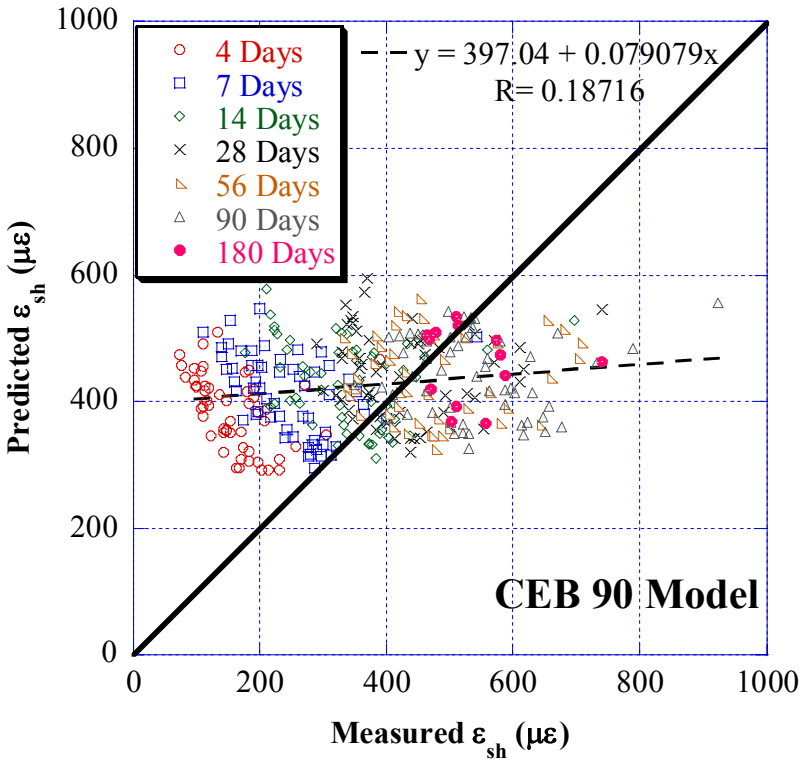

Fig. 3 Comparison of Predicted and Measured Shrinkage Strains for CEB 90 Models

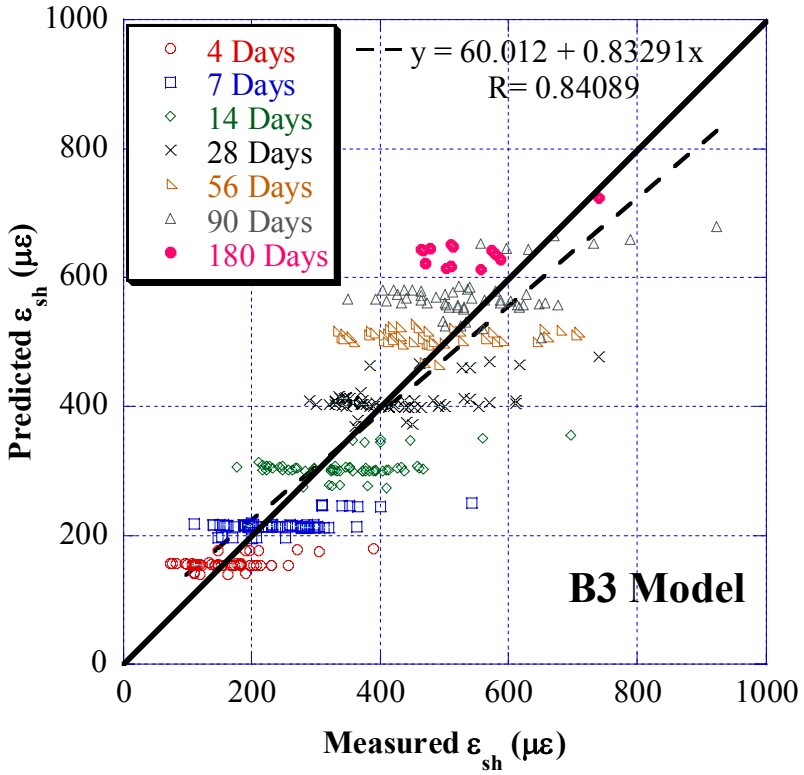

Fig. 4 Comparison of Predicted and Measured Shrinkage Strains for B3 Models

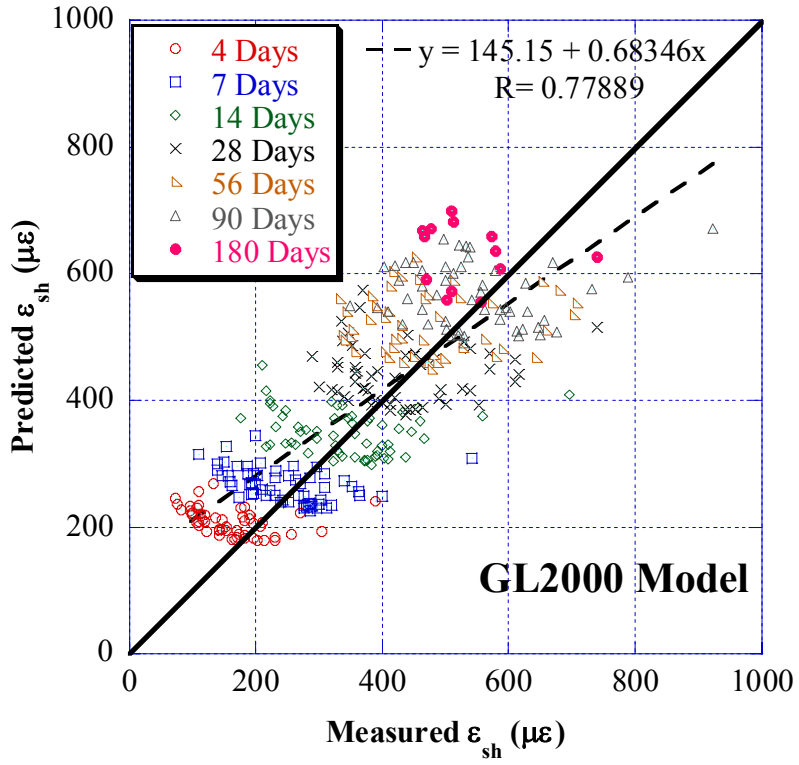

Fig. 5 Comparison of Predicted and Measured Shrinkage Strains for GL2000 Models

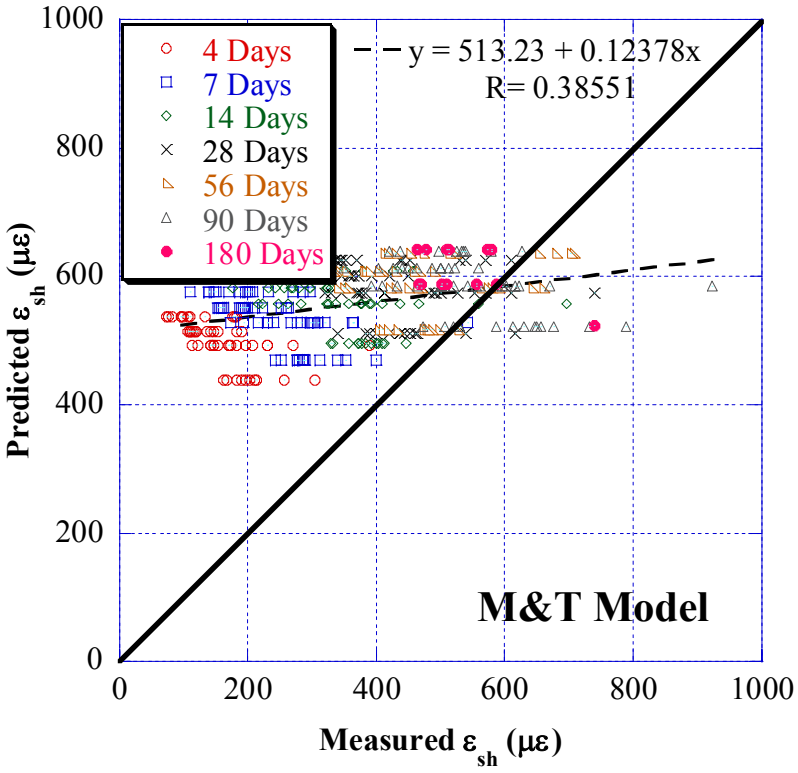

Fig. 6 Comparison of Predicted and Measured Shrinkage Strains for M&T Models.

The second objective of the paper is to determine the effect of pozzolans on autogenous shrinkage. Figs. 7 and 8 illustrate the autogenous shrinkage of the mix described in the experimental program. The mix containing fly ash shows the lowest autogenous shrinkage because fly ash slows down the hydration process and thus lowers autogenous shrinkage. Bentz et al explained this with more detail in the study of the influence of cement particle-size distribution on early-age autogenous strain and on stresses in cement-based materials; the rate of hydration increases with a finer particle size, causing higher autogenous shrinkage[19]. Because fly ash has a higher particle size, the hydration process in the concrete decreases, thus lowering the autogenous shrinkage.

As mentioned earlier, the autogenous shrinkage for HPC could be as high as the drying shrinkage (Fig. 8). Therefore, the fact that the drying shrinkage is in an acceptable range does not necessary mean the HPC will not crack. However, a solution is to simply cure the concrete immediately after pouring as revealed in another study by the authors[20].

Fig. 9 illustrates that autogenous shrinkage improves in concrete containing lightweight aggregates because of their high absorption percentage. As the concrete hydrates, the HPC with silica fume or with a low w/b ratio (or both) demands a lot of water. The water absorbed by the lightweight aggregate is released to satisfy the demand of water during the hydration process. Thus, the autogenous shrinkage is reduced. The autogenous shrinkage results were compared to M&T autogenous shrinkage model (Fig. 9). The model was observed to underpredict autogenous shrinkage of HPC. It should be noted that because the model only depends on the specimens' size and cement type, the predicted values are always the same for every mix.

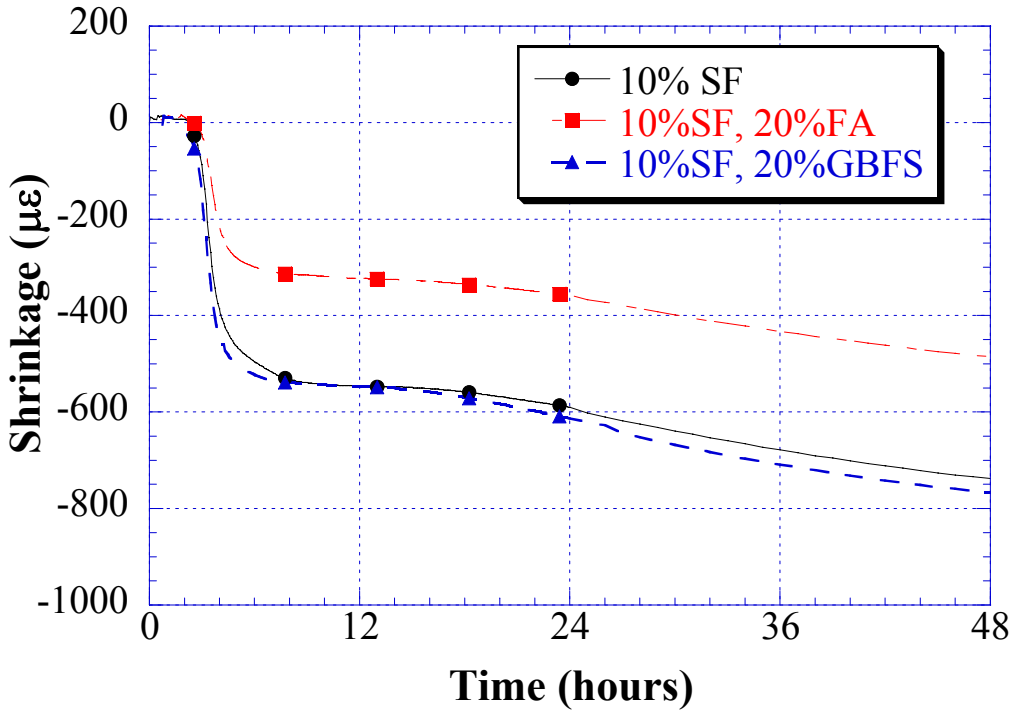

Fig. 7 Effect of Pozzolanic Material on Early-age (Autogenous) Shrinkage

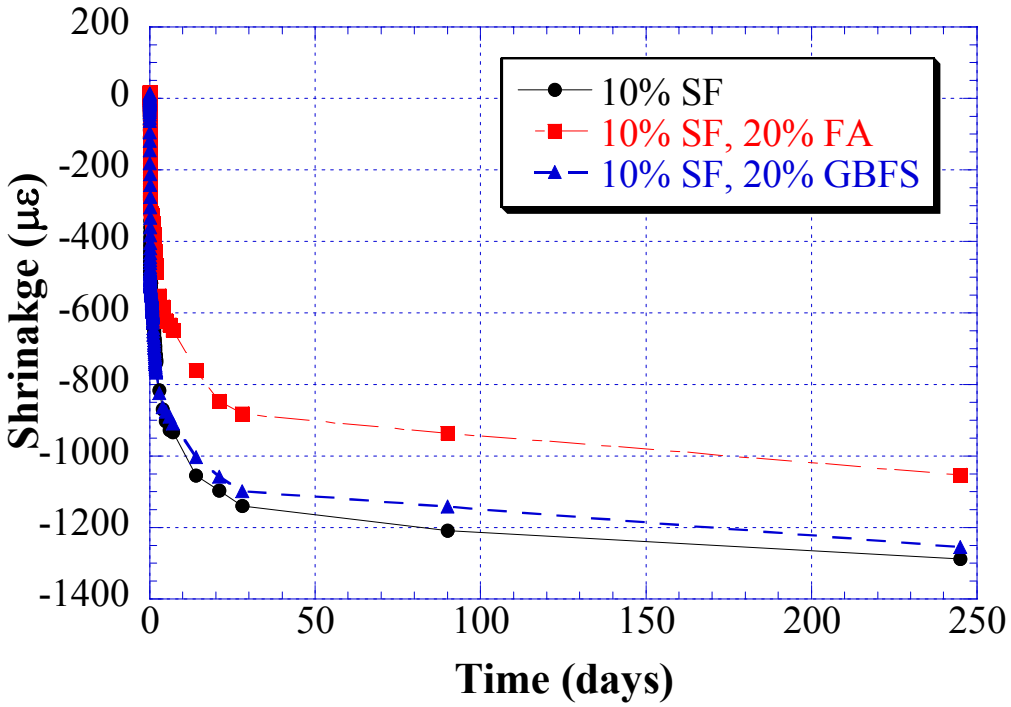

Fig. 8 Effect of Pozzolanic Material on Long-Term (Drying) Shrinkage

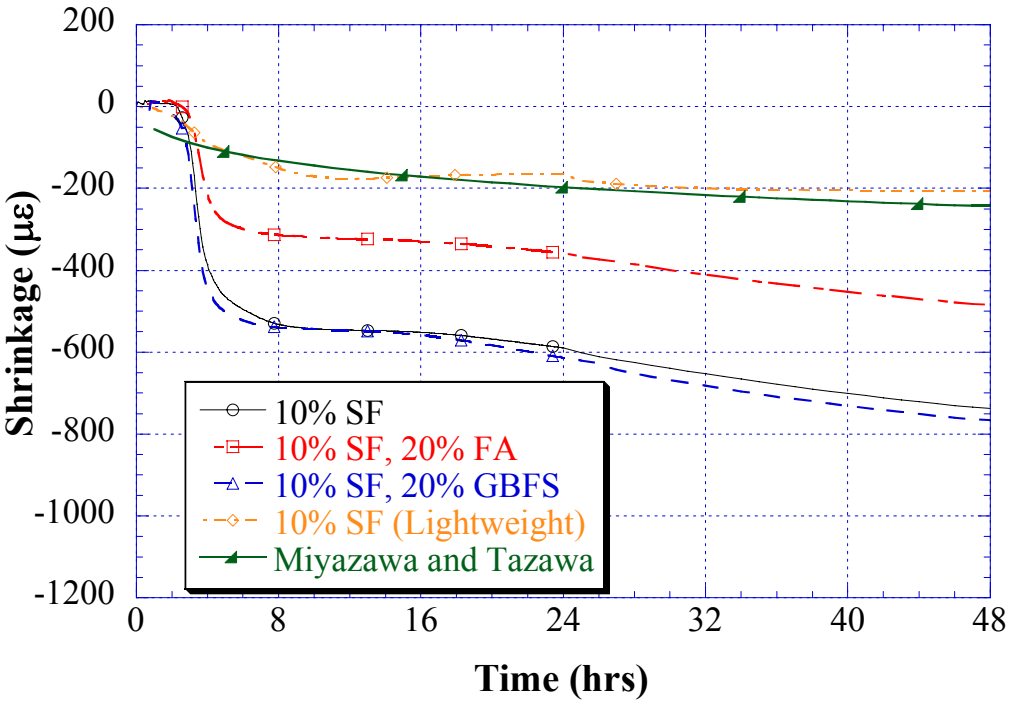

Fig. 9 Comparison of Miyazawa and Tazawa Autogenous Shrinkage Prediction Model with Measured Data.

CONCLUSION

This paper presents a comparison of the available shrinkage prediction models to measured data from tests performed on 61 HPC mixes. In addition, the effect of autogenous shrinkage is evaluated. From the study the following conclusions are drawn:

1. All observed shrinkage prediction models underpredict the long-term drying shrinkage. The B3 model has the best correlation with the measured values. The ACI 209 and GL 2000 models are also alternative models for accurately predicting shrinkage; however, the ACI 209 model underpredicts the shrinkage for air-dried concrete. The CEB 90 and M&T models do not provide a good correlation with the measured data.
2. The addition of fly ash to HPC will reduce both drying and autogenous shrinkage.
3. Autogenous shrinkage for HPC significantly contributes to the total shrinkage and could be as high as the drying shrinkage after 7 hours. Thus, autogenous shrinkage must be included in the shrinkage prediction models for HPC.
4. Lightweight aggregate reduces the autogenous shrinkage of HPC.

ACKNOWLEDGMENT

This study was funded by the New Jersey Department of Transportation (NJDOT) under a contract titled "Development of HPC Mix Designs for Transportation Structures in New Jersey." The findings expressed in this article are those of the authors and do not necessarily reflect the view of NJDOT. Its financial support and the technical assistance of the NJDOT staff are gratefully acknowledged. The authors also wish to acknowledge Lafarge, Separation Technology, Inc., and W.R. Grace for providing the raw materials.

REFERENCES

1. Ozyildirim, C., "HPC Bridge Decks in Virginia," Concrete International, February 1999, pp. 59 –60.
2. Waszczuk, C., and Juliano, M., "Application of HPC in a New Hampshire Bridge," Concrete International, February 1999, pp. 61 – 62.
3. Ralls, M.L., "Texas HPC Bridge Decks," Concrete International, February 1999, pp. 63 – 65.
4. Beacham, M., "HPC Bridge Deck in Nebraska," Concrete International, February 1999, pp. 66 – 68.
5. Streeter, D.A., "Developing High-Performance Concrete Mix for New York State Bridge Decks," Transportation Research Record, No. 1532, September 1996. pp. 60 –65.
6. Kanstad, T., Bjøntegaard, Ø., Sellevold, E.J., Hammer, T.A., and Fidjestøl, P. Effect of Silica Fume on early age crack sensitivity of High Performance Concrete. Proceedings of the International RILEM Workshop, Paris, France, October 2000.

7. Tazawa, E., and Miyazawa, S., "Influence of Cement and Admixture on Autogenous Shrinkage of Cement Paste," Cement and Concrete Research, Vol. 25, No. 2, 1995, pp. 281 – 287.
8. Igarashi, S., Bentur, A., Kovler, K., "Autogenous Shrinkage and Induced Restraining Stress in High-Strength Concretes," Cement and Concrete Research, Vol. 30, No. 11, 2001, pp. 1701 – 1707.
9. ACI Committee 209, *Prediction of creep, shrinkage and temperature effects in concrete structures.* Report No. ACI 209 R-92, ACI, 1992.
10. CEB-FIP, *CEB-FIP Model Code 1990: Design Code*. London, T Telford, 1993.
11. Bazant, Z.P., and Murphy, W.P. Creep and Shrinkage Prediction Model for Analysis and Design of Concrete Structures – Model B3. *Materials and Structures*, Vol. 28, No. 180, July 1995, pp. 357-365.
12. Bazant, Z.P., and Boweja, S. Justification and refinements of model B3 for concrete and shrinkage 1. Statistics and Sensitivity. *Materials and Structures*, Vol. 28, No. 181, Aug-Sept 1995, pp. 415-430.
13. Bazant, Z.P., and Boweja, S. Justification and refinements of model B3 for concrete and shrinkage 2. Updating and theoretical basis. *Materials and Structures*, Vol. 28, No. 182, October 1995, pp. 488-495.
14. Gardner, N.J., and Lockman, M. Design Provision for Drying Shrinkage and Creep of Normal-Strength Concrete. *ACI Material Journal,* Vol. 98, Mar-Apr 2001, pp. 159-167.
15. Miyazawa, S., and Tazawa, E. Prediction model for shrinkage of concrete including Autogenous shrinkage. Proceeding of the 6th International conference of CONCREEP-6@MIT, Cambridge, USA, August 2001.
16. Branson, D.E., and Christiason, M.L. Time-Dependent Concrete Properties related to Design-Strength and Elastic Properties, Creep, and Shrinkage. ACI Publication SP-76, 1982, pp. 257-277.
17. Muller, H.S. and Hillsdorf, H.K., "CEB Bulletin d' information, No. 199, Evaluation of the Time Dependent Behavior of Concrete, Summary Report on the work of general Task Group 9," Sept. 1990, p. 290.
18. Gardner, N.J., and Lockman, M. Design Provision for Drying Shrinkage and Creep of Normal-Strength Concrete. *ACI Material Journal,* Vol. 98, Mar-Apr 2001, pp. 159-167.
19. Bentz, D.P., Jensen, O.M., Hansen, K.K., Olesen, J.F., Stang, H., Haecker, C., "Influence of Cement Particle-Size Distribution on Early Age Autogenous Strains and Stresses in Cement-Based Materials," Journal of the American Ceramic Society, Vol. 84, No. 1, 2001, pp. 129 – 135.
20. Nassif, H.H., Suksawang, N., Mohammad, M., "Effect of Curing Methods on Early-Age and Drying Shrinkage of High Performance Concrete," Transportation Research Record, 2003, in press.